ELSEVIER

Surface Science 401 (1998) 248–260

surface science

A structural analysis of the Co(0001) surface and the early stages of the epitaxial growth of Cu on it

J.E. Prieto [a,*], Ch. Rath [b], S. Müller [b], R. Miranda [a], K. Heinz [b]

[a] *Dpto Fisica de la Materia Condensada, Universidad Autónoma de Madrid, Cantoblanco, E-28049 Madrid, Spain*
[b] *Lehrstuhl für Festkörperphysik, Universität Erlangen-Nürnberg, Staudtstr. 7, D-91058 Erlangen, Germany*

Received 20 June 1997; accepted for publication 3 December 1997

Abstract

The epitaxial growth of copper on Co(0001) was investigated by combined quantitative LEED and STM, including the clean surfaces Cu(111) and Co(0001). The mode of growth is a modified Stranski–Krastanov type, i.e. pseudomorphic and approximately layer-like up to four monolayers of copper; later on, three dimensional islands develop. The stacking of the copper adlayers is *exclusively* fcc from the very beginning, whereby the ABAB stacking on a given terrace of the substrate is continued as ABABca. Since there are also terraces with an ABA stacking, fcc-twins (e.g. ABAcb) develop in the Cu films. Whilst in the submonolayer coverage regime of copper the cobalt substrate remains hcp stacked, films with more than about two copper layers are found to have induced a stacking fault in the substrate corresponding to a registry shift of the uppermost cobalt layer. As indicated by the analysis of a film slightly above one monolayer coverage, the registry shift seems to be triggered when the terraces of the substrate are fully covered by copper whereby the rearrangement of atoms probably starts at the step edges. © 1998 Elsevier Science B.V. All rights reserved.

Keywords: Cobalt; Copper; Epitaxy; Low energy electron diffraction (LEED); Low index single crystal surfaces; Metal–metal interfaces; Scanning tunnelling microscopy (STM); Surface structure and morphology

1. Introduction

During the past few years numerous investigations have been carried out on the epitaxial growth of cobalt on surfaces of crystalline copper (e.g. Refs. [1–9]). This is partly due to the possibility of stabilizing at room temperature the fcc structure rather than the hcp equilibrium phase. For the early stages of the growth of Co on Cu(111) it has been found that structures in the range up to about two monolayers (ML) of cobalt mostly continue the fcc stacking of the substrate [6]. In this coverage range the cobalt islands are decorated [6] and even partly capped [5,6] with copper ejected from the substrate. At higher coverages the reaction with the substrate slows down and the hcp structure of bulk cobalt develops gradually [8]. Yet even for these thicker films the fcc structure of Co can be stabilized by capping the film with additional layers of copper forming a sandwich structure [8,9]. The same stabilization of fcc stacking has been found in Co/Cu superlattices [10–12]. So, it is obvious that cobalt follows to a large extent the fcc stacking when capped by copper or in a matrix with copper, as suggested by early data in Co–Cu powders [13].

From the structural point of view the question

* Corresponding author. Fax: (+34) 1 3973961; e-mail: jemilio@hobbes.fmc.uam.es

0039-6028/98/$19.00 © 1998 Elsevier Science B.V. All rights reserved.
PII: S0039-6028(97)01085-6

of which stacking is followed by copper when it is grown on hcp Co(0001) is raised. Trying to answer this question is the main issue of the present paper. At first glance one may be surprised that no such investigation exists, at least to the best of our knowledge. This is probably due to the difficulty in preparing a cobalt surface exhibiting only hcp(0001) domains. As it is well known, cobalt undergoes a structural (martensitic) phase transition to the fcc structure when heated beyond 420°C. Although in principle this transition is reversible, fcc domains usually remain on the surface when the crystal is cooled down again. It may also be by this fact that only one quantitative surface structure determination seems to exist for clean Co(0001) [14].

In this paper we present structural analyses of Cu/Co(0001) for various copper coverages using quantitative low energy electron diffraction (LEED) and scanning tunneling microscopy (STM). In order to have immediate reference to the structural parameters of the substrate we also carried out a structure determination of clean Co(0001). As the two existing structure determinations of clean Cu(111) report a small contraction [15,16] and expansion [17] of the top layer distance, we include this surface in our analyses for consistency reasons.

The paper is organized as follows. In Section 2 we describe the preparation of both the clean crystal surfaces and the ultrathin films and give details of the LEED and STM measurements. This is followed in Section 3 by an outline of the full dynamical intensity calculations and the retrieval of the correct structure. Section 4 presents the structural results achieved for clean Co(0001) and Cu(111), and we concentrate on the structure and morphology of the epitaxial films in Section 5. Eventually, a conclusive discussion of the results is presented.

2. Sample preparation and data acquisition

The experiments were carried out in a standard UHV chamber equipped with a rear-view four-grids LEED optics which also served as a spectrometer for Auger electron spectroscopy (AES).

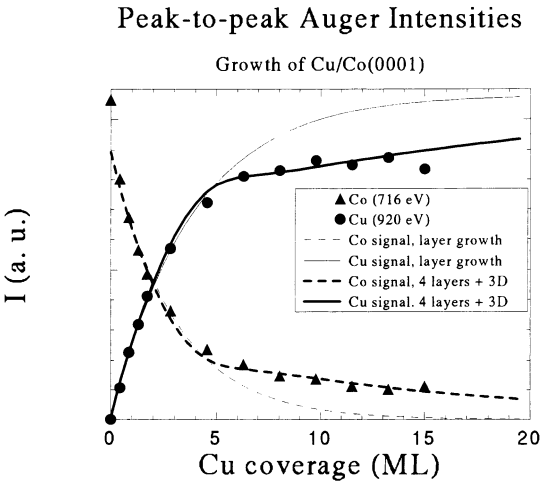

Fig. 1. Evolution of the intensities of the high-energy Auger peaks of Co(716 eV) and Cu(920 eV) during deposition of Cu on Co(0001) at room temperature. Thin lines are calculated for a layer-like growth with the damping parameters taken from Ref. [8]. This model fits the data up to a coverage of 4 ML. From this coverage on they are best fitted with larger effective mean free paths (heavy lines) pointing to 3D islanding.

The Co(0001) sample was cleaned by repeated argon ion sputtering followed by extended annealing at 350°C, whereby care was taken not to cross the transition temperature of about 420°C to fcc cobalt. Occasionally, the sample was exposed to oxygen during annealing in order to eliminate the carbon. As a result of the mild cleaning procedure imposed to avoid the structural phase transition of crystalline cobalt, some impurities may have remained in the surface region. The sample cleaning was considered complete when the C(272 eV)/Co(53 eV) Auger peak ratio was less than 1/200, which corresponds to about 4% of a ML.

Deposition of copper was made from a reservoir by evaporation through electron bombardment at a rate of about 1 ML min^{-1}. The sample was kept at room temperature (RT) during deposition. The developing LEED patterns were always 1×1 with sixfold symmetry. The change in peak-to-peak height of the high-energy Auger peaks of Co(716 eV) and Cu(920 eV) with deposition time is shown in Fig. 1. There are two distinct regimes of growth characterized by different attenuations of the AES signals. The evolution of the peaks is

consistent with the expected exponential dependence for homogeneous covering of the substrate until 4 ML of Cu. No parameters have been fitted in this region of the plot except for one overall scale factor; the attenuation factors and relative sensitivities used are those quoted below. After the first 4 ML the decay (increase) of the Co (Cu) signal proceeds at a much smaller rate. Note, for instance, that after 15 ML of Cu the signal from the Co substrate is still detected. Although this may be influenced by the non-continuous deposition mode needed for recording the Auger spectra, the most natural interpretation is a change in the mode of growth from layer-like to strong three-dimensional islanding, i.e. a Stranski–Krastanov-like growth mode with a 4 ML thick wetting layer. The thickness of the wetting layer (4 ML) is confirmed by the disappearance of the low energy Auger peak of Co approximately at this coverage. A three-dimensional growth is the known mode of growth of Cu on Cu(111) [18], a situation that our system should resemble from a certain coverage on.

In the following we will concentrate on the coverage region below 4 ML. The deposited Cu coverage was determined from the ratio of the high energy Auger peaks, $Co_{716}/Cu_{920} = S\alpha^n_{Co}/(1-\alpha^n_{Cu})$ where $S = Co(716\,eV)/Cu(920\,eV)$ is the ratio of signals from the bulk crystals determined to be in the same conditions $S = 0.83$. The quantity $\alpha^n_{Co} = (\alpha_{Co})^n$ describes the experimental [8] attenuation of the Co signal across n layers of Cu ($\alpha_{Co} = 0.72$), whilst α^n_{Cu} stands for the corresponding attenuation of the Cu signal ($\alpha_{Cu} = 0.77$). The attenuation factor for a given Auger peak derives from the inelastic mean free path λ of electrons of the corresponding energy as $\alpha = \exp(-a/0.8\lambda)$, whereby a is the monolayer thickness. The accuracy of the coverage determination is estimated to be about ± 0.2 ML. Three films were prepared with thicknesses of nominally 0.7, 1.2 and 2.8 ML as determined by AES. Within the limits of error these values are consistent with the coverages of about 0.8, 1.25 and 2.7 ML later determined by the LEED analysis.

Information with respect to the morphology of the films, to which LEED is largely blind, was retrieved from STM. Images were recorded at RT with a home-made STM [3] operated in the constant current mode.

LEED intensity versus energy spectra, $I(E)$, were measured at RT using a video-based and commercially available automated image data acquisition system, AIDA-PC, described in detail elsewhere [19,20]. The normal incidence of the primary beam was adjusted carefully by quantitative comparison of symmetrically equivalent spectra via the Pendry R-factor [21]. Finally, the degenerate spectra were averaged in order to improve the data quality with respect to residual sample misalignment, to possible inhomogeneities of the LEED screen and to noise.

3. Intensity calculations and structural search

For the intensity calculations full dynamical programs were used [22,23]. A total of 11 phase shifts proved to be sufficient to describe the atomic electron scattering up to the maximum energy of 400 eV used in the analyses. They were calculated relativistically, spin averaged and corrected for isotropic thermal vibrations using appropriate Debye temperatures. The latter were fixed for subsurface layers (Co: 445 K; Cu: 343 K [24]) and varied in the course of the structure determination for surface layers. As usual, layer diffraction matrices were calculated by matrix inversion in angular momentum space and layers were stacked using the layer doubling scheme, whereby an optical potential V_{0i} was used to simulate the electron attenuation. In view of the epitaxial growth to be investigated, the in-plane lattice parameter a_p was also varied in addition to the interlayer distances d_{ik}. Owing to the exact translational symmetry assumed in the LEED codes, a_p has to be the same for all layers (film and substrate) within one domain. If this parameter is not the same for all layers an average value will result in the best fit for this domain. For the film systems we made allowance for different structural domains with different stacking sequences of the first few layers. With respect to the latter, LEED is rather sensitive as shown explicitly for the epitaxial growth of copper and cobalt recently [8,25]. Because of the similar atomic scattering of cobalt and copper (see

Ref. [8]) unambiguous elemental identification of atoms was possible only in the first two layers. The structural parameters and relative weights of the various domains were determined using a structural search algorithm on the basis of a modified random sampling procedure [26] whereby the Pendry R-factor [21] was used for the quantitative comparison of experimental and calculated model intensities. The variance of this R-factor, $\mathrm{var}(R) = R_{\min}\,(8V_{0i}/\Delta E)^{1/2}$ with $R_{\min}$ the best-fit R-factor and ΔE the energy width of the data base, was used to estimate error limits owing to statistical errors of the measurement [21].

As all patterns (except that of clean copper) exhibit sixfold symmetry, the resulting data base of intensities of non-degenerate beams is comparably small, i.e. typically in the range of $\Delta E \approx 500$–550 eV (compared with $\Delta E = 1070$ eV for the threefold symmetric clean copper). On first glance this is unfavourable with respect to $\mathrm{var}(R)$, i.e. to the resulting error limits. Yet, it will turn out that our analyses are characterized by very low best-fit R-factors which bring the error limits back to low values. Nevertheless, in view of the restricted data base it is worth focussing for a moment on the redundancy issue. A single peak in a spectrum, which is usually considered as an independent piece of structural information, has a width of about $4V_{0i} \approx 20$ eV. So, with a total data base of 500 eV a maximum of 25 pieces of structural information can be retrieved. However, in this case no redundancy is left and therefore the structure determination is not on very safe grounds in view of both experimental and calculated data being, to some unknown extent, affected by statistical and systematic errors. For the clean surfaces, for which five structural parameters (three interlayer distances, the bulk distance and the lateral lattice parameter) will be determined below, our data base provides a redundancy factor of five for Co (10 for Cu) which certainly is more than enough. When two different structural domains are present on the surface, the 11 parameters to be determined reduce the redundancy factor to about two. Although this is lower than the factor of three which is usually believed to be on the safe side, we are inclined to accept this under the condition that the structural parameters, in particular for deeper layers, are reasonable, i.e. come close to the bulk values. It will turn out that this is the case. Nevertheless, in order to reduce the number of free parameters we decided to take advantage of our knowledge of the interlayer distances of the clean cobalt surface, assuming they remain unchanged in the uncovered domains in the 0.8 and 1.25 ML films. This brought the number of free parameters down to six for the former and 12 for the latter case, where three domains were found by STM and also turned out to be necessary in the fit. For this case, we additionally set the spacings d_{45} and all deeper layers as well as the in-plane lattice parameter a_p to the values of bulk Co. This brought the number of parameters down to eight. At higher coverages we again included the variation of d_{45} and of a_p corresponding to a total of 11 parameters, i.e. to the edge of being reasonable by the above arguments. Even then, the values obtained for deep layers are reasonable, meaning that they can be set at bulk values and the fit will not change appreciably. As a test, we increased the number of parameters and checked for variation in the results. It turned out that the number of parameters could be increased up to 20 without making the former determined parameters leave the error limit range. We have to remark that there is independent information from STM concerning the existence of different domains, i.e. the surface morphology. Agreement of the domain analysis by LEED with the STM images (and AES data) will be essential in order to place trust in the structure determined.

4. The structures of the clean Co(0001) and Cu(111) surfaces

Excellent fits could be achieved for the clean surfaces of the cobalt and copper crystals with minimum Pendry R-factors $R_{\min}(\mathrm{Co}) = 0.080$ and $R_{\min}(\mathrm{Cu}) = 0.117$. At least for cobalt this was somewhat unexpected in view of the difficulties in preparing a crystalline clean hcp surface. A representative large scale STM image of clean Co(0001) exhibits terraces of widely different sizes as displayed in Fig. 2. The terraces are separated by steps with different atomic heights (1, 2 and 3

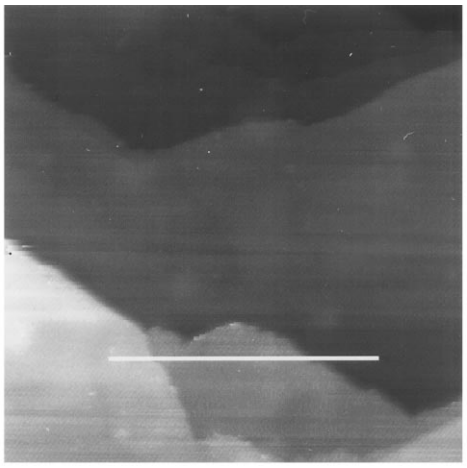

Fig. 2. STM topographic image of the clean Co(0001) surface (100×100 nm^2). The profile along the line in the image shows a mono- and a biatomic step.

interlayer distances) allowing ABA and BAB stacking sequences to exist close to the surface, which accounts for the observed six-fold rotational symmetry of the diffraction pattern. Table 1 exhibits the best-fit structural parameters for the two surfaces resulting from the optimization of the first three interlayer distances $d_{i,i+1}$ ($i=1,2,3$), of subsequent interlayer distances d_b assumed to be all the same, of the in-plane lattice parameter a_p and of the surface Debye temperature Θ_S. The data base widths ΔE and the variances of the Pendry R-factor, from which the error limits are deduced, are given as well. It is worth noting that, as mentioned above, in spite of the comparatively reduced values of ΔE, the error limits are rather

Table 1
Structural parameters derived by the LEED analyses for Co(0001) and Cu(111). For d_b and a_p also the ideal bulk values are given as taken from the literature

Clean surfaces	Co(0001)	Cu(111)
d_{12} (Å)	1.99 ± 0.02	2.07 ± 0.01
d_{23} (Å)	2.06 ± 0.04	2.08 ± 0.02
d_{34} (Å)	2.01 ± 0.06	2.08 ± 0.03
d_b (Å)	2.05 ± 0.05	2.09 ± 0.04
d_b (Å)/Lit.	2.047	2.087
a_p (Å)	2.51 ± 0.06	$2.55^{+0.02}_{-0.03}$
a_p (Å)/Lit.	2.507	2.556
Θ_S (K)	235^{+25}_{-15}	280^{+60}_{-40}
R_{min}	0.080	0.110
ΔE (eV)	550	1070
var(R)	0.022	0.020

small. This is a consequence of the small minimum R-factors achieved in each case.

The values derived for the in-plane lattice parameters a_p and the bulk interlayer distances d_b agree with the literature values for the bulk materials nearly exactly. As usual, the surface Debye temperatures are considerably reduced with respect to the bulk values. Also in agreement with the literature, and frequently found for close packed metal surfaces [27], the Cu(111) surface is practically bulk terminated, i.e. the 0.8% contraction of the top layer distance is just outside the limits of error. On the contrary, the best-fit for Co(0001) exhibits a contraction of the first interlayer distance by about $\Delta d_{12}/d_b \approx -3\pm1\%$. The second layer distance turns out to be bulk-like, the third one surprisingly seems again to be contracted ($\Delta d_{34}/d_b \approx -2\pm2\%$), but this latter feature is not outside the limits of error. It is worth noting, however, that our recent LEED structure determination of a 5 ML Co(0001) film grown on Cu(111) [8] exhibited, outside the statistical limits of error, practically the same relaxation features as the crystal surface investigated in the present case. As this earlier analysis was based on an independently measured data set, taken on a completely different surface system, we feel encouraged to take the oscillatory behaviour observed for Co(0001) seriously. The only other existing quantitative structure determination of Co(0001) reports a bulk-like terminated surface [14]. Yet, as it was based on visual comparison of experimental and

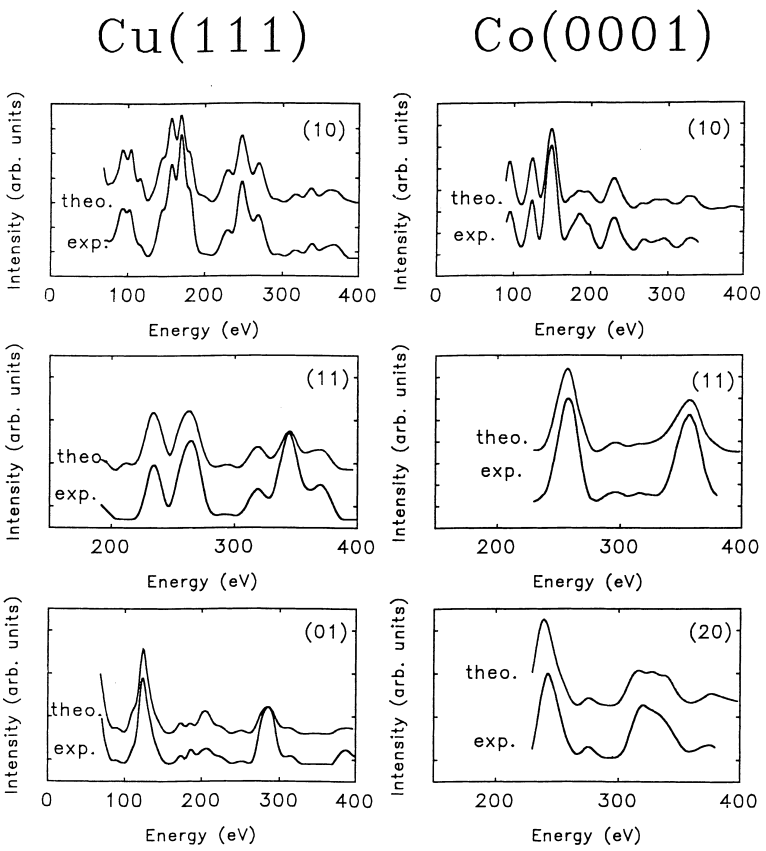

Fig. 3. Experimental and best-fit model intensities for clean Cu(111) (left) and Co(0001) (right) for a selection of diffracted beams.

calculated LEED spectra, the weak relaxation may have been overlooked.

The excellent quality of the theory–experiment fit achieved for the two surfaces can also be judged by visual impression in Fig. 3 where a selection of spectra is displayed. The comparison of curves for Co and for Cu illustrates the strong sensitivity of LEED with respect to the layer stacking [25]. The spectra are quite different in spite of the similar lattice parameters and scattering strengths of the two elements.

5. Structure and morphology of ultrathin Cu films on Co(0001)

5.1. Submonolayer Cu coverages (0.8 ML)

Deposition of 0.4 ML of Cu on Co(0001) produces STM images like the one shown in Fig. 4. Rather large and irregularly shaped monolayer-high islands of Cu grow on the cobalt terraces. The low density of islands indicate an efficient diffusion of the Cu adatoms on the terraces, while the irregular shape of the island edges speaks in favour of a reduced adatom mobility along the steps. In some cases, portions of the islands touch the steps, but contrary to the mirror system, Co/Cu(111) [3,6], there is not a preferential decoration of the steps. A LEED analysis has been carried out for a Cu film of 0.8 ML thickness as estimated by AES. It included the variation of the first four interlayer distances for domains covered by copper whilst deeper spacings were kept fixed at the bulk value of Co ($d_b = 2.05$ Å). As mentioned in Section 4, the layer spacings of the uncovered cobalt were kept fixed at the best-fit values determined from the clean surface. In view of the different in-plane lattice parameters of clean Co

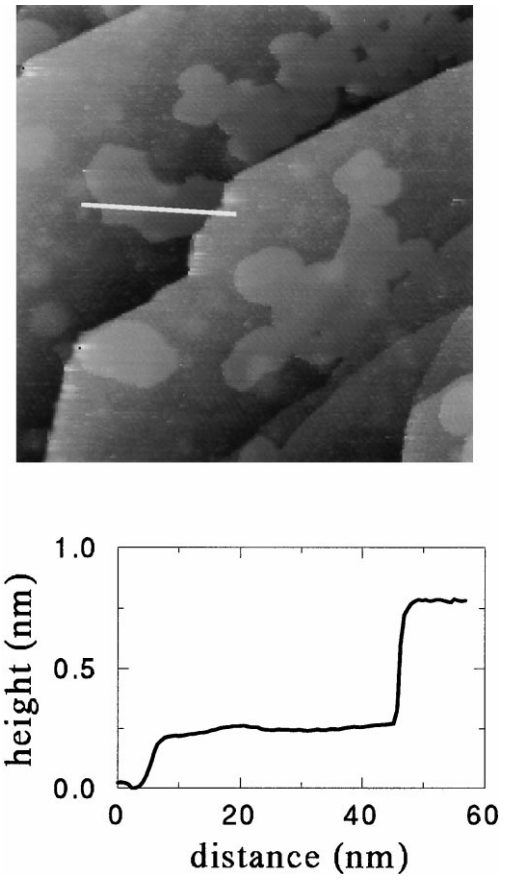

Fig. 4. STM image after deposition of 0.4 ML of Cu at room temperature on Co(0001). The size of the image is $170 \times 170\ nm^2$. Large and compact but irregularly shaped monoatomic-high islands form on the terraces. The profile runs through a Cu island and a multiatomic step of the substrate.

and Cu, this quantity (a_p) was also varied. As the coverage of the surface with Cu is known only approximately from AES, the relative weights of covered and uncovered domains were also varied, whereby also the existence of domains with Cu double layers was tested. Copper was allowed both to continue the hcp stacking of the substrate or to exhibit a stacking fault at the interface, whereby again two domains are possible according to the two different step-separated domains present on the clean surface. In view of the fact that copper was found to induce a change from hcp to fcc stacking when additionally deposited on a 5 ML hcp Co film grown on Cu(111) [8], we also tested for possible stacking faults induced in the Co substrate. The surface Debye temperature of the top copper layer was also allowed to vary, not affecting, however, the structural results. Of course, only such domain combinations were considered which reproduced the six-fold rotational symmetry of the LEED pattern observed in the experiment.

The best-fit ($R_{min}=0.098$) results for 80% (error limits $\pm 10\%$) of the surface covered with a single layer of copper whose stacking on the substrate is of fcc type. The two different atomic terminations of the hcp terraces (ABAB and ABA) induce the existence of two domains in the Cu monolayer (ABABC and ABAC), which are in fact local fcc twins of each other. Hcp stacked copper layers (ABAB or ABABA) can be excluded within error limits of $\pm 15\%$. No stacking fault is induced in the substrate below copper (the assumption of a stacking fault brings the R-factor up to $R_p=0.29$ and simultaneously yields unreasonable interlayer spacings). Population of a second copper layer is found to be negligible within an error of 10% of a ML, which indicates a rather extended initial wetting of the substrate and is consistent with approximate layer-by-layer growth. Some 20% of the Co surface remains uncovered. The best-fit and measured spectra of the (10) and (11) beams are displayed in the lower part of Fig. 5 where, additionally, the respective spectra of clean Co are given for comparison. The strong modifications of

Table 2
Structural parameters for the best-fit of the 0.8 ML Cu/Co(0001) film (20% of the surface is uncovered)

Cu/Co(0001) (low coverage: 0.8 ML)	Cu single layer (fcc stacked)
Weight (%)	80 ± 10
d_{12} (Å)	2.10 ± 0.02
d_{23} (Å)	2.00 ± 0.04
d_{34} (Å)	2.06 ± 0.07
d_{45} (Å)	2.03 ± 0.10
a_p (Å)	2.51 ± 0.03
Θ_S (K)	260 ± 40
R_{min}	0.098
ΔE (eV)	520
var(R)	0.03

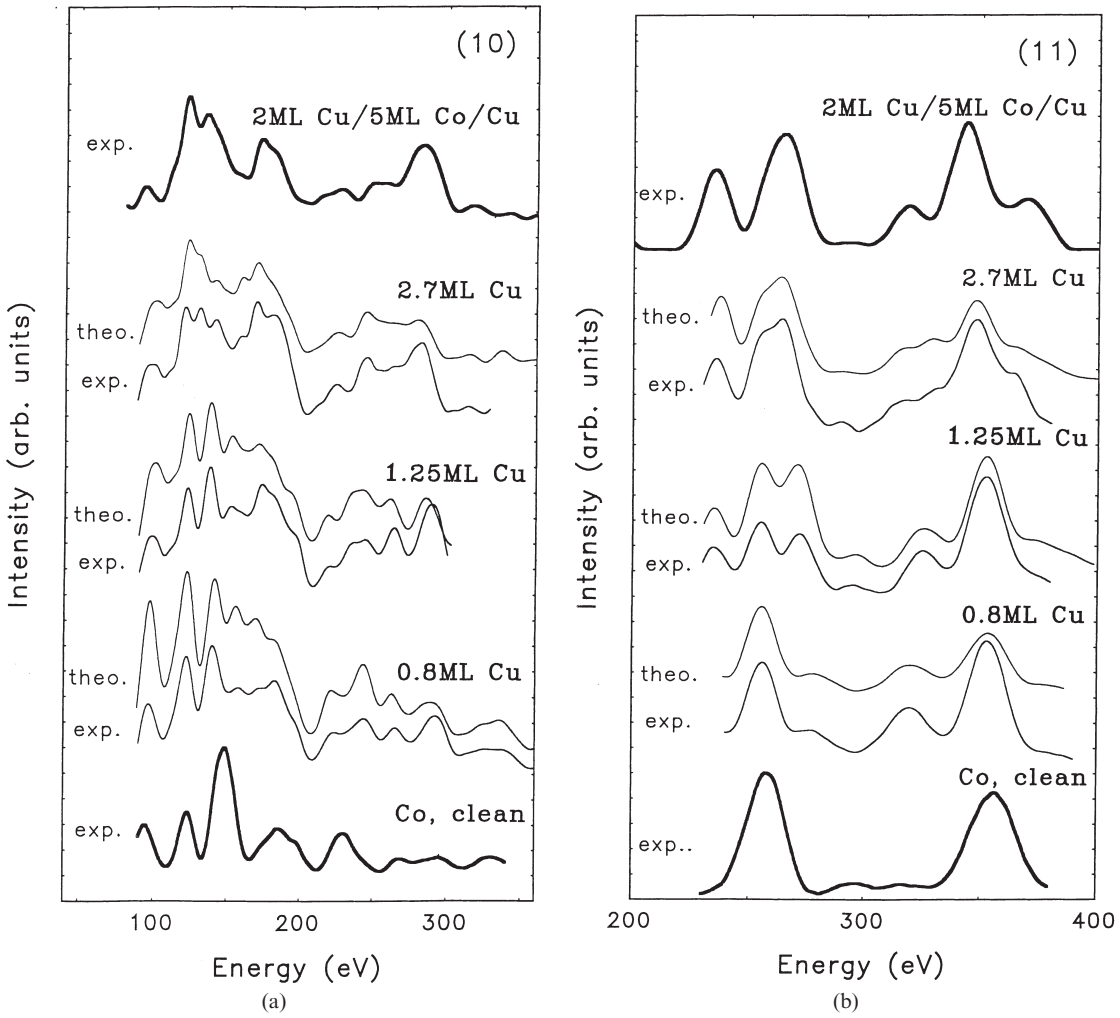

Fig. 5. Experimental and best-fit model intensities of the 10 and 11 beams compared for different film thicknesses and the clean surfaces as indicated.

the film spectra compared to the data of the clean surface are indicative of the fcc stacking of copper. The Cu coverage determined by the LEED analysis is within the limits of error (± 0.2 ML) in agreement with AES. Both the coverage and the absence of double layers are consistent with STM images like that shown in Fig. 6. In summary, for this coverage copper does not follow the ABAB stacking of the substrate, nor are there stacking faults induced in the cobalt substrate. Instead copper locates exclusively on the local fcc adsorption site.

All parameters are displayed in Table 2 including the error limits. The in-plane lattice parameter remains that of cobalt. The distance between the copper layer and the substrate (2.10 Å) is in reasonable agreement with the interlayer spacing in the Cu(111) surface (2.09 Å). Layer spacings within cobalt are practically bulk-like within the limits of error. An exception might be the first cobalt interlayer distance which still seems to be contracted as in the clean surface. Yet, as the respective error limits almost cover the bulk value this conclusion is rather uncertain.

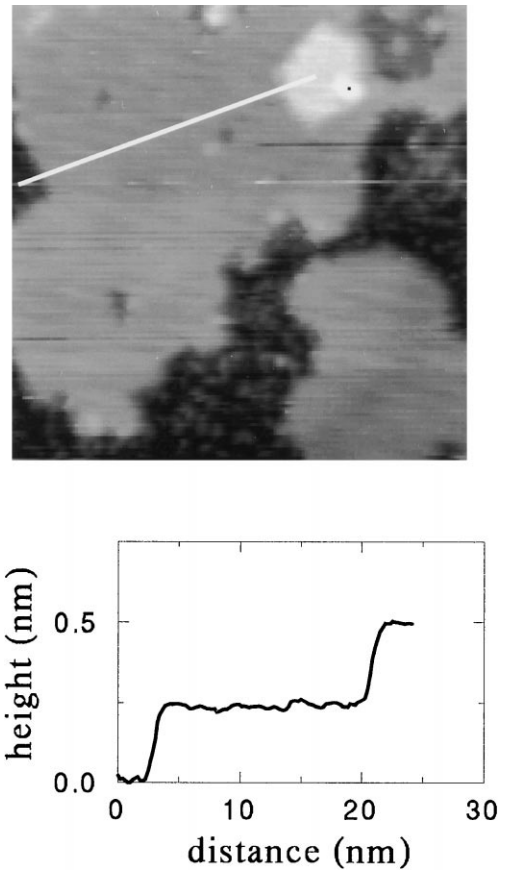

Fig. 6. STM image of a 0.8 ML film on Co(0001). A large monolayer-high Cu island with a small second layer Cu island is seen together with a scan profile through both.

5.2. High copper coverage (2.7 ML)

With further copper deposited, the spectra resemble more and more those of a clean, but twinned fcc copper crystal. This is apparent for a film of 2.7 ML coverage whose (10) and (11) spectra are compared to those of a sandwich arrangement of 2 ML Cu/5 ML Co/Cu in the top panels of Fig. 5. In earlier investigations this sandwich film was found to be practically completely fcc stacked [8] and our 2.7 ML Cu/Co film exhibits many similar intensity peaks indicative of the dominance of fcc stacking. Yet, some features arising from the Co have also remained as expected from the not completely buried substrate. The quantitative multilayer analysis of the 2.7 ML film, which yields a minimum R-factor $=0.07$, tells that there are only domains with three Cu adlayers ($70\pm20\%$) and two Cu adlayers ($30\pm20\%$) of pseudomorphic (compressed) copper. This is again consistent with an approximate layer-by-layer growth, at least within LEED sensitivity, possibly promoted by compressive strain as reported for Ag/Pt(111) [28]. The domain weights determined by the intensity analysis correspond to a coverage of 2.7 ML which is consistent with the AES data. The stacking sequence of Cu is strictly fcc in both domains. Moreover, the fit shows without any doubt that at least the first five layers of the sample have an fcc stacking. Therefore, below the Cu film, part of the cobalt substrate has modified the stacking to fcc. Without considering this Cu-induced stacking fault in the Co substrate, the R-factor would raise to $R=0.2$, i.e. well beyond the variance level $R_{\min}+\mathrm{var}(R)=0.092$. So, the existence of stacking faults in the Co substrate is outside the statistical limits of error. Table 3 displays the best-fit values of all parameters varied. The lateral lattice parameter a_p is still that of cobalt, i.e. no lateral relaxation towards the copper lattice parameter has taken place yet, and the film growth is still strictly pseudomorphic. This relaxation could be related with the end of approximate layer-by-layer growth at 4 ML. The interlayer distances are slightly larger than that of Cu(111),

Table 3
Structural parameters for the best-fit of the 2.7 ML Cu/Co(0001) film (sf = stacking fault)

Cu/Co(0001) (high coverage: 2.7 ML)	Domains with	
	Three layers Cu (fcc stacked)	Two layers Cu (fcc stacked)
Weight (%)	70 ± 20	30 ± 20
d_{12} (Å)	2.10 ± 0.02	2.09 ± 0.03
d_{23} (Å)	2.14 ± 0.04	2.11 ± 0.05
d_{34} (Å)	2.09 ± 0.07	2.09 ± 0.09
d_{45} (Å)	2.08 ± 0.11	$2.02+0.14$
a_p (Å)	2.51 ± 0.03	2.51 ± 0.03
Θ_S (K)	260^{+60}_{-40}	
$R_{\min}$	0.07	
ΔE (eV)	500	
var(R)	0.022	

consistent with the tetragonal distortion related to an unchanged value of a_p in the film.

5.3. Medium copper coverage (1.25 ML)

In view of the copper-induced stacking fault detected in the cobalt substrate at 2.7 ML coverage and the absence of such a stacking fault in the submonolayer coverage range, it is interesting to investigate the case of an intermediate coverage. Fig. 7 shows a characteristic STM image of Co(0001) covered by 1.25 ML of Cu. There are white "blobs" that occupy 0.05 ML and are probably due to Cu nucleated at defects or contamination. Beside their small extension, they do not seem to influence the growth significantly, since no differences can be seen between regions near or far from them in the image. Copper islands cover 90% of the surface. Their rounded edges do not follow the steps of the original surface which, in fact, cannot be recognized in the image – a rather unusual observation for growth of metal on metal at the level of a monolayer of deposited material. The population of the second layer is about 30%. This distribution of layers is consistent with approximate layer growth and at variance with the Poisson distribution of exposed levels expected for three-dimensional growth at this total coverage. We allowed in the LEED fit for domains with triple, double and single copper layers in addition to uncovered cobalt areas. Only the first three interlayer distances as well as the stacking of layers (hcp or fcc) were varied including stacking faults possibly induced in the substrate. In view of the fact that both for the low and high coverage the growth was found to be strictly pseudomorphic, this was also assumed for the present case, i.e. the lateral lattice parameter was kept fixed at $a_p = 2.51$ Å. For the structure of uncovered cobalt again the best-fit values of the clean surface were used. As the existence of copper triple layers could be ruled out, this setting implies the fit of eight parameters including the relative weights of domains.

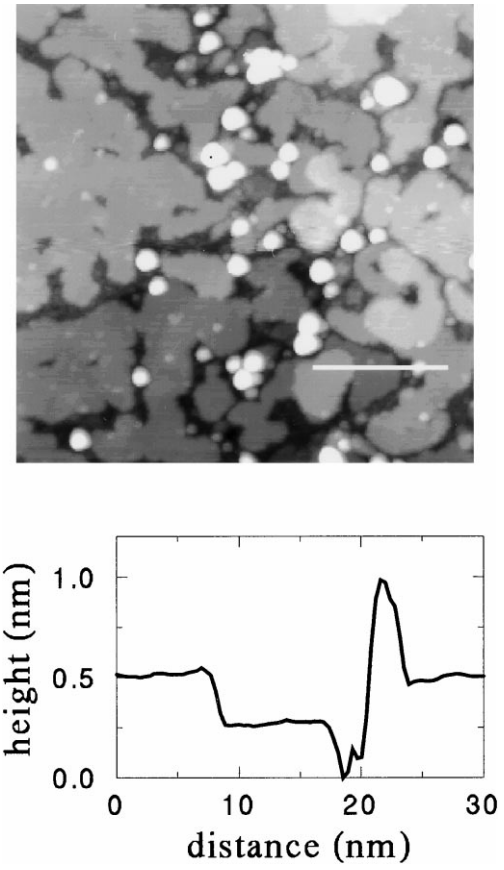

Fig. 7. STM image of 1.25 ML Cu/Co(0001). The size of the image is 100×100 nm^2. There are regions of local Cu coverages of 1 ML (60% of the surface) and 2 ML (30%). The profile runs through the edge of a second layer Cu island and a white "blob" probably related to residual contamination. Note that it is no longer possible to recognize the step structure of the original surface.

The best fit ($R_{min} = 0.084$) develops for the following structural arrangement. As much as 85% of the surface exhibits at least 4 ML with fcc stacking. Only double ($40 \pm 20\%$) and single ($45 \pm 20\%$) Cu layers exist, in agreement within error bars with the distribution found by STM. The weight of the uncovered cobalt patches is 0.15 ML, yet the respective error limits are about as large as that. All this is equivalent to a coverage of 1.25 ML in agreement with the estimation from AES. The stacking of copper in the single and double layer is exclusively fcc. Underneath the single-layer fraction ($45 \pm 20\%$) of the Cu film, the best-fit requires a stacking fault induced in the cobalt substrate. As given in Table 4, the distances between copper layers and between copper and cobalt layers at the interface are close to the copper

Table 4
Structural parameters for the best-fit of the 1.25 ML Cu/Co(0001) film (sf = stacking fault, 15% of the surface is uncovered)

Cu/Co(0001) (medium coverage: 1.25 ML)	Domains with	
	Cu double layer fcc stacked (no sf in substrate)	Cu single layer fcc stacked (sf in substrate)
Weight	40 ± 20	45 ± 20
d_{12} (Å)	2.09 ± 0.02	2.09 ± 0.02
d_{23} (Å)	2.14 ± 0.04	2.05 ± 0.05
d_{34} (Å)	2.02 ± 0.07	2.03 ± 0.08
d_b (Å)	2.047 (not varied)	2.047 (not varied)
a_p (Å)	2.51 (not varied)	2.51 (not varied)
Θ_s(K)	240^{+60}_{-20}	
R_{min}	0.084	
ΔE (eV)	510	
var(R)	0.026	

bulk value. The best-fit spectra, displayed for the (10) and (11) beams in the middle panels of Fig. 5, demonstrate that practically all the details of the experimental data are reproduced, consistent with the low R-factor.

If the theory–experiment fit is enforced to include a stacking fault in the substrate below both the single and double layer of Cu, the R-factor increases to 0.106. Although this simultaneously yields some unrealistic interlayer distances in the substrate, we cannot fully discard this model on the basis of R-factors. Yet, enforcing that the stacking fault develops only below the copper double layer (i.e. not below the single layer) yields an $R = 0.194$, i.e. a model well outside the error limits. On the other hand, without any consideration of the induced stacking fault, the best-fit R-factor would be 0.133. Alhough this is above the variance level ($R_{min} + \mathrm{var}(R) = 0.110$) and some unrealistic layer distances and distributions appear, the respective spectra are also very close to the experiment (equivalent to the still low R-factor) and one might feel uncertain about the appearance of the stacking fault. Yet, there are no doubts about its existence in the high coverage region (2.7 ML). As a consequence, there must be some critical coverage or coverage region at or in which the development of the stacking fault is triggered. This could coincide with the completion of a monolayer.

6. Discussion and conclusions

The main structural results of our investigations, which for each coverage considered were retrieved on the basis of a very good theory–experiment fit and consistent with STM images, can be summarized as follows:

(1) The clean surfaces exhibit no surprises. The Cu(111) surface is practically bulk-like terminated, whilst Co(0001) shows a weak multilayer relaxation with (as usual) a maximum change of the interlayer distance between the two uppermost layers ($\Delta d_{12}/d_b \approx -3 \pm 1\%$).

(2) The growth of the first four layers of copper on Co(0001) is approximately layer-like. It is also strictly pseudomorphic at least up to the third layer, i.e. copper accommodates to the lateral lattice parameter of cobalt, which is 1.5% smaller than the copper value. It appears that this reduction is partly compensated by slightly increased vertical interlayer distances in the epitaxial film.

(3) Copper does not follow the substrate's hcp stacking and grows with an fcc stacking sequence from the very beginning. Hereby, fcc stacking means that the ABAB sequence of the substrate is continued as ABABc, ABABca, etc. On the other type of terraces of the substrate the film growth follows the local fcc sequence (ABAcb) so that fcc twin-domains develop.

(4) At a coverage of above one monolayer (here 1.25 ML), the copper adatoms induce a stacking fault in the top layer of part of the cobalt crystal, which extends to the full substrate for larger Cu thicknesses (here 2.7 ML).

Evidently, copper grows on Co(0001) exclusively with fcc stacking. It even induces stacking faults in the cobalt substrate forcing its surface region to be partly fcc. This can be understood by the following, admittedly speculative, scenario. Copper adatoms arriving on the clean surface do not adsorb preferentially at the steps, but rather tend to form epitaxial (fcc stacked) islands on the

terraces, where there is no stacking conflict with the atoms of the neighbour upward step, as displayed in Fig. 4. With further copper deposition second layer islands start to form, and by the time that the first copper layer is completed a stacking conflict appears at step edges. As the stacking fault energy in cobalt is very low (20 ergs cm^{-2}) [29], this conflict can be solved by the top cobalt layer in the upper terrace or at least part of it undergoing a registry shift to fcc. As a result of this process and because this registry shift will surely not be homogeneous along the step direction due to kinks, statistical distribution of Cu islands or other defects, the step structure of the original surface is not reproduced by the growing film and cannot be recognised in the corresponding STM images (Fig. 7). Of course, the registry shift is equivalent to the introduction of a stacking fault in the cobalt substrate (with partial dislocations in the surface plane). Locally, this process is in favour of suppressing the growth of fcc twin-domains of equal weight. However, at the next terrace the registry shift will be in the opposite direction maintaining on average the same weight of different twins. Probably, the stacking fault partially relaxes the strain induced by the compressed pseudomorphic Cu film. The amount of material in the cobalt substrate with modified fcc stacking increases with the thickness of Cu deposited in the range explored here. The induction of stacking faults seems to be an intrinsic feature of the copper growth on Co(0001). It can be understood from the low energetic cost of a stacking fault in Co and from the fact that the chemical potential of a stacking fault as a function of the distance from a bimetallic interface shows a Friedel-like oscillatory behaviour that can favour its appearance right at the interface [30]. This is in agreement with recent investigations of the growth of cobalt films on Cu(111) capped by additional layers of copper, either by depositing Cu directly onto them [8] or by annealing the structure in order to favour Cu diffusion to the surface [9]. In both cases, the capping Cu layers were found to induce changes in the stacking sequence of the cobalt film. Furthermore, it is also consistent with the reported observation of predominant fcc stacking in Co/Cu superlattices [10–12].

In conclusion, our investigations by combined quantitative LEED and STM show that the epitaxial growth of Cu on Co(0001) is strictly pseudomorphic for the first few layers and dominated by practically exclusive fcc stacking of the growing film layers. The influence of copper with respect to stacking is even large enough to induce a registry shift of the top cobalt layer, when the corresponding terrace is fully covered by copper. This is equivalent to the induction of a stacking fault probably started at the substrate's step edges.

Acknowledgements

The authors are indebted to the Spanish Ministerio de Educación y Ciencia and Deutscher Akademischer Austauschdienst (DAAD) through the programme "Acciones Integradas" granting scientific exchange visits. The work has also been financially supported by the DGICyT through grant PB94.1527. Klaus Heinz thanks the Instituto de Ciencia de Materiales "Nicolás Cabrera" for additional financial support.

References

[1] B.P. Tonner, Z.-L. Han, J. Zhang, Phys. Rev. B 47 (1993) 9723.
[2] M.T. Kief, W.F. Egelhof, Jr., Phys. Rev. B 47 (1993) 10785.
[3] J. de la Figuera, J.E. Prieto, C. Ocal, R. Miranda, Phys. Rev. B 47 (1993) 13043.
[4] V. Scheuch, K. Potthast, B. Voigtländer, H.P. Bonzel, Surf. Sci. 318 (1994) 115.
[5] A. Rabe, N. Memmel, A. Steltenpohl, Th. Fauster, Phys. Rev. Lett. 73 (1994) 2728.
[6] J. de la Figuera, J.E. Prieto, G. Kostka, S. Müller, C. Ocal, R. Miranda, K. Heinz, Surf. Sci. 349 (1996) L139.
[7] S. Müller, G. Kostka, T. Schäfer, J. de la Figuera, J.E. Prieto, C. Ocal, R. Miranda, K. Heinz, K. Müller, Surf. Sci. 352–354 (1996) 46.
[8] Ch. Rath, J.E. Prieto, S. Müller, R. Miranda, K. Heinz, Phys. Rev. B 55 (1997) 10791.
[9] Y. Wang, X.W. Li, J.F. Xia, H. Ji, Y. Yang, H. Gul Bahar, S.C. Wu, R.G. Zhao, Surf. Sci. 375 (1997) 226.
[10] F.J. Lamelas, C.H. Lee, H. He, W. Vavra, R. Clarke, Phys. Rev. B 40 (1989) 5837.
[11] K. Le Dang, P. Veillet, H. He, F.J. Lamelas, C.H. Lee, R. Clarke, Phys. Rev. B 41 (1990) 12902.

[12] H.A.M. de Gronckel, K. Kopinga, W.J.M. de Jonge, P. Panissod, J.P. Schillé, F.J.A. den Broeder, Phys. Rev. B 44 (1991) 9100.
[13] V.A. Phillips, Trans: Met. Soc. AIME 230 (1964) 967.
[14] B.W. Lee, R. Alsenz, A. Ignatiev, M.A. Van Hove, Phys. Rev. B 17 (1978) 1510.
[15] S.Å. Lindgren, L. Walldén, J. Rundgren, P. Westrin, Phys. Rev. B 29 (1984) 576.
[16] S. Tear, K. Röll, M. Prutton, J. Phys. C 14 (1981) 3297.
[17] I. Bartos, P. Jaros, A. Barbieri, M.A. Van Hove, W.F. Chun, Q. Cal, M.S. Altman, Surf. Rev. Lett. 2 (1995) 477.
[18] W. Wulfhekel, N.N. Lipkin, J. Kliewer, G. Rosenfeld, L.C. Jorritsma, B. Poelsema, G. Comsa, Surf. Sci. 348 (1996) 227.
[19] K. Heinz, Rep. Prog. Phys. 58 (1995) 637.
[20] H. Wedler, K. Heinz, Vakuum Forsch. Prax. 7 (1995) 107.
[21] J.B. Pendry, J. Phys. C 13 (1980) 937.
[22] J.B. Pendry, Low Energy Electron Diffraction, Academic Press, London, 1974.
[23] M.A. Van Hove, S.Y. Tong, Surface Crystallography by LEED, Springer, Berlin, 1979.
[24] E. Gray (Ed.), American Institute of Physics Handbook, McGraw-Hill, New York, 1972.
[25] H. Ascolani, J.R. Cerdá, P.L. de Andrés, J.J. de Miguel, R. Miranda, K. Heinz, Surf Sci. 345 (1996) 320.
[26] M. Kottcke, K. Heinz, Surf. Sci. 376 (1997) 352.
[27] NIST Surf. Struct. Database 2.0 (1995), Nat. Inst. Stand. Technol., Gaithersbury, USA.
[28] H. Roder, K. Bromann, K. Kern, Surf. Sci. 376 (1997) 13.
[29] F.R.N. Nabarro, Theory of Crystal Dislocations, Oxford University Press, New York, 1967, p. 248
[30] A.C. Redfield, A.M. Zangwill, Phys. Rev. B 34 (1986) 1378.